Soil Dynamics and Earthquake Engineering 47 (2013) 117–131

Contents lists available at SciVerse ScienceDirect

Soil Dynamics and Earthquake Engineering

journal homepage: www.elsevier.com/locate/soildyn

Performance of bridges with seismic isolation bearings during the Maule earthquake, Chile

Mauricio Sarrazin *, Ofelia Moroni, Carlos Neira, Braian Venegas

University of Chile, Civil Engineering, Blanco Encalada 2002, Santiago, Chile

ARTICLE INFO

Article history:
Received 14 November 2011
Received in revised form
5 April 2012
Accepted 23 June 2012
Available online 21 July 2012

ABSTRACT

On February 27, 2010 an earthquake of magnitude M_w=8.8, with epicenter in Cobquecura, Maule region, hit the central part of Chile. After the earthquake, a tsunami occurred that caused heavy casualties and damage to buildings and infrastructure. In particular, 4.5% of the overpasses located in the affected region suffered some type of damage and 25 bridges and several pedestrian bridges collapsed. At that time, there were about a dozen bridges with seismic isolation bearings in Chile, two of which were instrumented with accelerometer networks: the Marga Marga Bridge, located in Viña del Mar, and an elevated section of the Metro Line 5 in Santiago, at approximately 300 km and 400 km from the epicenter, respectively. This paper analyzes the acceleration records obtained at these instrumented structures and studies the effect of the seismic isolation on their dynamic response. The beneficial effect of the isolation system, especially in the longitudinal direction, is apparent. In addition, some flaws in the collapsed bridges are described.

1. Introduction

An 8.8 magnitude earthquake struck central Chile at 3:34 AM on February 27th, 2010, followed by a tsunami that swept the coastline between Llolleo and Lebu, nearly 700 km apart. The epicenter was located 35 km deep, off the coast of Cobquecura, Maule Region. According to seismic data the rupture zone was 500 km long and 150 wide [1]. This area is one of the most densely populated in Chile and concentrates the majority of the industrial facilities in the country, excluding mining. The damage to buildings, industries and road works were substantial.

The area is instrumented with a network of broadband seismometers and strong motion accelerometers, thus a large number of records at the epicentral area was obtained [1,2]. The earthquake lasted nearly 140 s with a strong motion part of 40–50 s. The largest horizontal acceleration was recorded by the Melipilla station (0.78 g), about 50 km from the coast and more than 200 km away from the epicenter. This station also recorded high accelerations during the 1985 earthquake. However the damage in Melipilla city was quite modest as compared with places closer to the epicenter, where lower accelerations were recorded.

In the last 15 years, many concession roads have been built or renovated in Chile, which include several major bridges. Following the worldwide trend [3], most of the important bridges have some seismic protection system consisting of natural rubber or neoprene isolators, friction bearings and/or energy dissipation devices. In the disaster zone there are two bridges with seismic isolation support that are instrumented with accelerometer networks: Marga Marga Bridge, located in Viña del Mar, at approximately 300 km from the epicenter and, a viaduct section of the Metro Line 5 in Santiago, some 400 km away from the epicenter. The acceleration records obtained at both structures are analyzed in this paper. The effect that the seismic isolation had on the dynamic response of the structures is also assessed. This type of analysis has been performed for bridges in other countries [4,5]; however the high magnitude of the earthquake and the local soil conditions are unprecedented and make this research of interest. Failures of highway bridges and crosswalks at various locations in Chile are also described.

2. Description of damaged bridges

Most bridges in Chile are composed of simply supported steel or reinforced concrete beams, with transverse diaphragms that connect locally the beams over the piers and/or at the abutments. In addition, vertical anchorage rods called "seismic bars" are provided at the supports (see Fig. 1). This practice changed around the year 2000, when the use of precast prestressed concrete beams was massified, and the transverse diaphragms

* Corresponding author. Tel.: +56 2231 8406; fax: +56 2334 7194.
E-mail address: sarrazin@ing.uchile.cl (M. Sarrazin).

0267-7261/$ - see front matter © 2012 Elsevier Ltd. All rights reserved.
http://dx.doi.org/10.1016/j.soildyn.2012.06.019

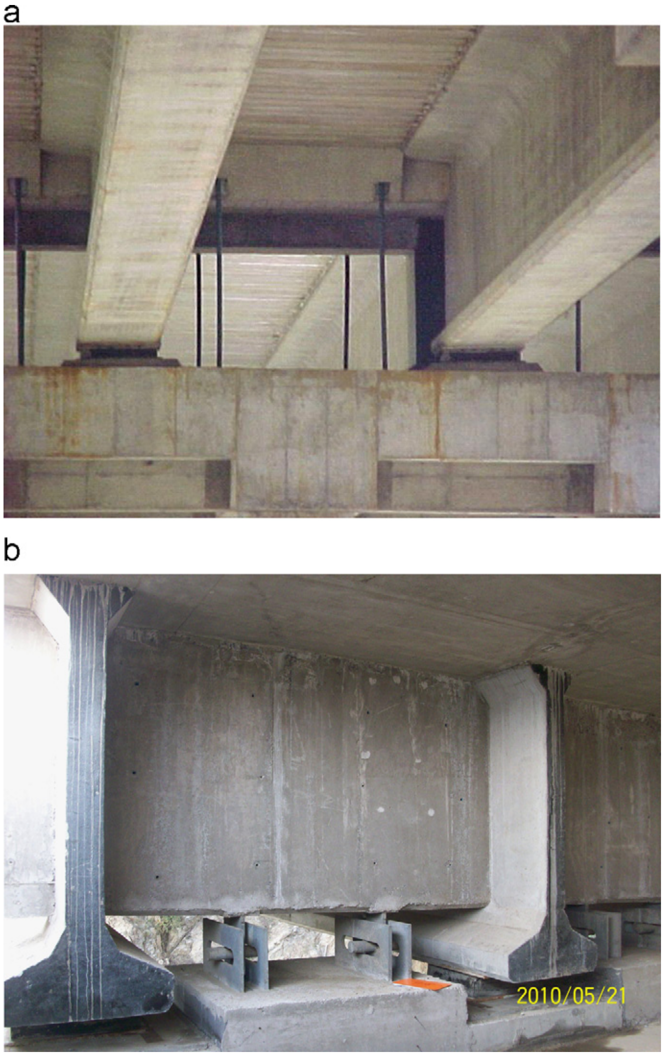

Fig. 1. "Seismic bars" and transverse diaphragms in typical simply supported bridge.

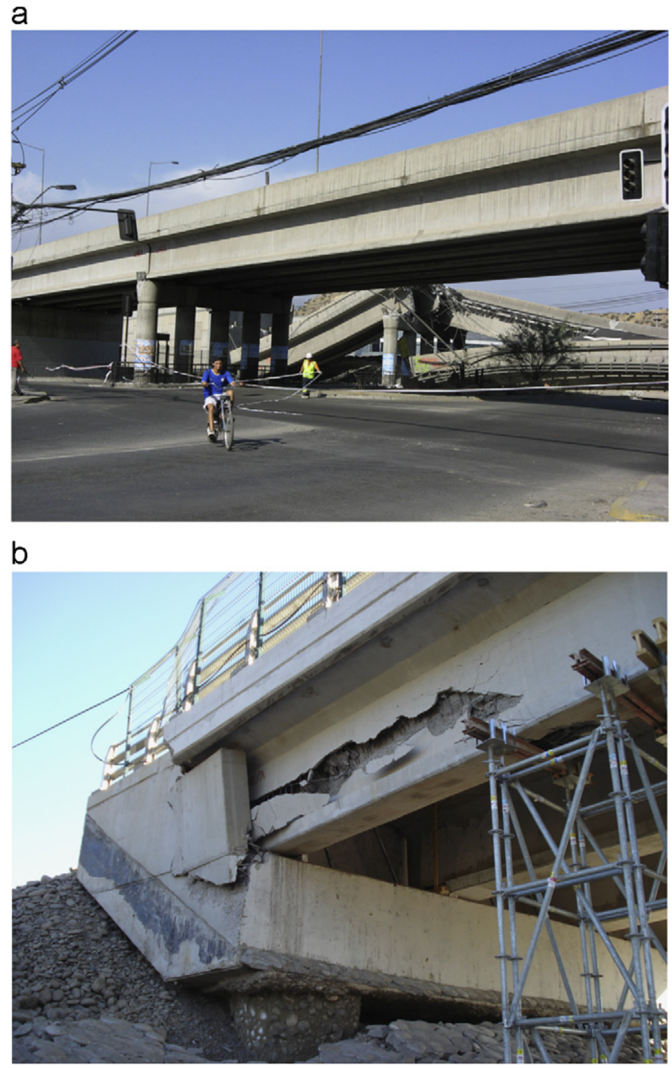

Fig. 2. (a) Vespucio Norte Overpass. Insufficient steel stoppers.(b) Overpass near Rancagua.

were eliminated. Instead of them, steel or reinforced concrete stoppers were considered at the bottom flange of the beams in the transverse direction.

Most bridges with large spans and tall piers are equipped with seismic isolation and/or dissipation devices. Using ambient vibration records and FFT analysis, Moroni et al. [6] determined in some of them the fundamental frequencies and equivalent damping. In the horizontal direction, frequencies varied between 0.68 Hz and 1.46 Hz and the equivalent damping between 1% and 4.4%

About 4.5% of the overpasses failed due to the earthquake and 25 bridges collapsed, 10 of them on public roads and 15 in privately managed toll roads [7]. A detailed description of the failures of 32 bridges, several of them of the skew type, was reported by Yen et al. [8]. It is believed that the skewed shape and the lack of transverse diaphragm over the abutments were the main cause of the collapse of the overpasses. After the earthquake experience, the Ministry of Public Works decided that the use of transverse diaphragms should be compulsory. The damage to highways around Santiago, as Vespucio Norte and South East Highway, both operated by private agencies, had a big economic impact. Other badly affected areas were the village of Hospital and the Rancagua By-Pass. Fig. 2a shows a collapsed overpass in Vespucio Norte where the steel side stoppers were insufficient to hold the beam flanges. Other factors that contributed to the damage were the lack of vertical restraint bars at the supports and the small size of the supporting area. Fig. 2b shows a damaged overpass with a significant lateral displacement of the superstructure that broke the reinforced concrete stoppers. In addition, local amplification of seismic waves and poor soil quality was reported in all these sites.

Three bridges over the Bio Bio River, connecting the city of Concepción to the south, partially collapsed (see Fig. 3a). Liquefaction and lateral spreading of the soil could explain such damage. Between Curico and Talca, over the Claro River, an old bridge built in 1890 collapsed. It was a 117 m long bridge, formed by 7 masonry arches of about 25 m height. This bridge (Fig. 3b) had been declared a National Monument a few years earlier.

All seismically isolated bridges, with the exception of Cardinal Silva Henriquez Bridge in Constitución, had good performance. Some of them can be seen in Fig. 4. Detailed damage in Cardinal Silva Henriquez Bridge is described in [8]. The main damage was a lateral displacement of the supporting plates that produced failure of the stoppers. The welded connection of the beams to one of the abutments was also fractured. Despite the damage, light vehicles were allowed to cross the bridge while it was repaired.

Fig. 3. (a) Bridge in Concepción.(b) Collapsed Claro river bridge.

3. Marga Marga Bridge

3.1. Description

The Marga Marga Bridge, built in 1996, is located in Viña del Mar. A view and a general scheme are shown in Fig. 5. The superstructure consists of a reinforced concrete deck, 0.27 m thick and 18 m wide, and 4 continuous steel I-beams, which rest on 36 rubber isolators located at the two abutments and the 7 piers. The piers have a hollow rectangular section of 2×10 m, 0.25 m thick. The deck can move only longitudinally at the abutments. There are reinforced concrete transverse elements connecting the steel beams at both ends. All spans, except the southernmost one, are 50 m long. The total length of the bridge is 383 m. Pier height varies between 22 and 32 m. Groups of ten one-meter diameter piles, with depths ranging from 14 to 31 m, bear piers C2–C6, whereas the piers C1, C7 and the abutments are supported directly on rock. A complete description of this bridge is in [9].

Isolators' section varies depending on the vertical load applied. They are 0.85×0.55 m over the piers, 0.5×0.7 m at the north abutment and 0.5×0.5 m at the south abutment. The required shear modulus of the rubber for 50% strain was 0.75 ± 0.05 MPa with an equivalent damping of 8 to10%. This was verified during the construction process by testing rubber samples in direct shear and each of the 36 rubber bearings.

The monitoring system of the bridge consists of 24 sensors placed at the following locations: free field-valley, free field-rock, base and top of pier C4, north and south abutments and several positions on the deck, as shown in Fig. 6. The top of Fig. 6 shows the deck with the sensors in the transverse and longitudinal directions and the bottom shows pier C4 with sensors 2, 5, 8 and 14 that measure in the vertical direction. Using this network for ambient vibrations, frequencies in longitudinal (L) and transverse (T) direction, as well as damping of the superstructure were determined (see Table 1). This table also shows the corresponding frequencies and equivalent damping obtained from the July 24, 2001 earthquake records. At the deck, the predominant frequencies in both horizontal directions were reduced considerably during the strong motion interval of the earthquake, while the equivalent damping in longitudinal direction increased, reaching up to 15%.

Ambient vibrations were measured using seismometers at the ground, at the bottom of pier C4 and at the valley, 20 m apart to the west of pier C4. Predominant frequencies of 1.3 Hz in both horizontal directions and 1.8 Hz in the vertical direction were identified. Subsequently, frequencies in horizontal direction of 1.2 Hz at the valley and 4.4 Hz on the rock at the south abutment were obtained from moderate seismic records using Nakamura's method. [10].

3.2. Maule earthquake records

Figs. 7, 8 and 9 show the acceleration records, in fractions of g, obtained during the February 27th, 2010 earthquake in the longitudinal, transverse and vertical directions, respectively. Peak accelerations are listed at the right end of each diagram. There is a significant reduction of accelerations in the longitudinal direction between the pier and the deck and also between the abutments and the deck. Accelerations at the south abutment are much larger than at the north one, although both sites may be classified as hard soils. The differences in topographic conditions between one abutment and the other could explain the differences in accelerations. There is also a considerable change in the dominant frequency of the different records. Acceleration on the deck at sensors 7, 18 and 12 are quite similar, indicating nearly a rigid body motion in the longitudinal direction.

In the transverse direction, the accelerations are of the same order of magnitude at the deck and at the piers, but almost twice the "free-field values". Peak accelerations at the deck reached the largest values, 1.9 g and 1.4 g at the north and south abutments, respectively. This fact could be explained by the existence of friction between the deck and the lateral stoppers. For moderate earthquakes, it has been observed that the horizontal accelerations are generally higher at the valley than at the base of the pier, which seems to indicate that the piles attenuate the ground motion. However, this effect was not observed this time.

There was a significant reduction between the free field and the base of the pier in the vertical direction (first two graphs of Fig. 9), probably due to the effect of the piles that are embedded in the soil to reach harder layers. On the deck, the amplification in the vertical direction is apparent, especially in sensor 15, located on top of pier C6. Differences between sensors 8 and 14 may indicate some torsion of the deck. Finally, it is confirmed that the bridge is exposed to differential support motions, so this effect should be taken in account in any analytical study of this bridge.

Elastic acceleration spectra (5% damping) of the longitudinal and transverse valley free field ground motions and the design spectrum are shown in Fig. 10. Although the design spectrum is lower than the spectra obtained from the records, the bridge performed as expected at the design stage.

The square of the Fourier spectra of the records, in both horizontal directions, are shown in Figs. 11 and 12. The free field-valley motions have large peaks, with amplitudes of the

Fig. 4. Undamaged isolated bridges: Marga Marga Bridge, Cartagena Viaduct, El Bosque Radial Nororiente, Américo Vespucio.

Fig. 5. General view, Marga Marga Bridge Viña del Mar.

order of 40 around 1.21 Hz, and 50 around 0.95–1.05 Hz in the longitudinal and transverse directions, respectively. In both horizontal directions there are small peaks of the order of 10 around 1.9 and 2.4 to 2.6 Hz. The motions at the bottom of the pier are very similar to the free-field motion, with larger amplitudes at these same frequencies. At the top of the pier, in the longitudinal direction, the amplitude at 1.21 Hz increases up to 150, while in the transverse direction the largest amplitude (around 80) is between 2.4–2.6 Hz. The motion at the free field and at the pier for frequencies above 5 Hz show very little energy. The motion at the deck in the longitudinal direction shows very small peak amplitudes: 3.2 for 0.42 Hz, 2.1 for 0.7 Hz and 4 for 6.1 Hz. The first peak of the square of the Fourier spectrum on the deck is associated with the natural frequency of the deck sliding as a rigid body on the bearings.

These results show clearly the beneficial effect of the isolation bearings on the response in the longitudinal direction, in which the deck is free to move. The motion in the transverse direction experiences a significant change in its frequency content and their amplitudes are reduced with respect to the top of the pier to less than half. Note that in this direction there are stoppers that prevent the motion at the abutments.

Predominant frequencies were obtained using three different time intervals along the duration of the records, which were filtered using a Butterworth band pass filter between 0.2 and 20 Hz. As could be expected, the frequencies changed with time, demonstrating the nonlinear behavior of the isolation bearings. The natural frequencies are shown in Table 2. The longitudinal frequency at the deck presented a significant reduction as compared to previous earthquakes and is quite close to the value used at the design phase (0.5 Hz). This table also shows the equivalent damping obtained from the strong motion segments of the records. Dai et al. [11] studied the effect of the stiffness of the

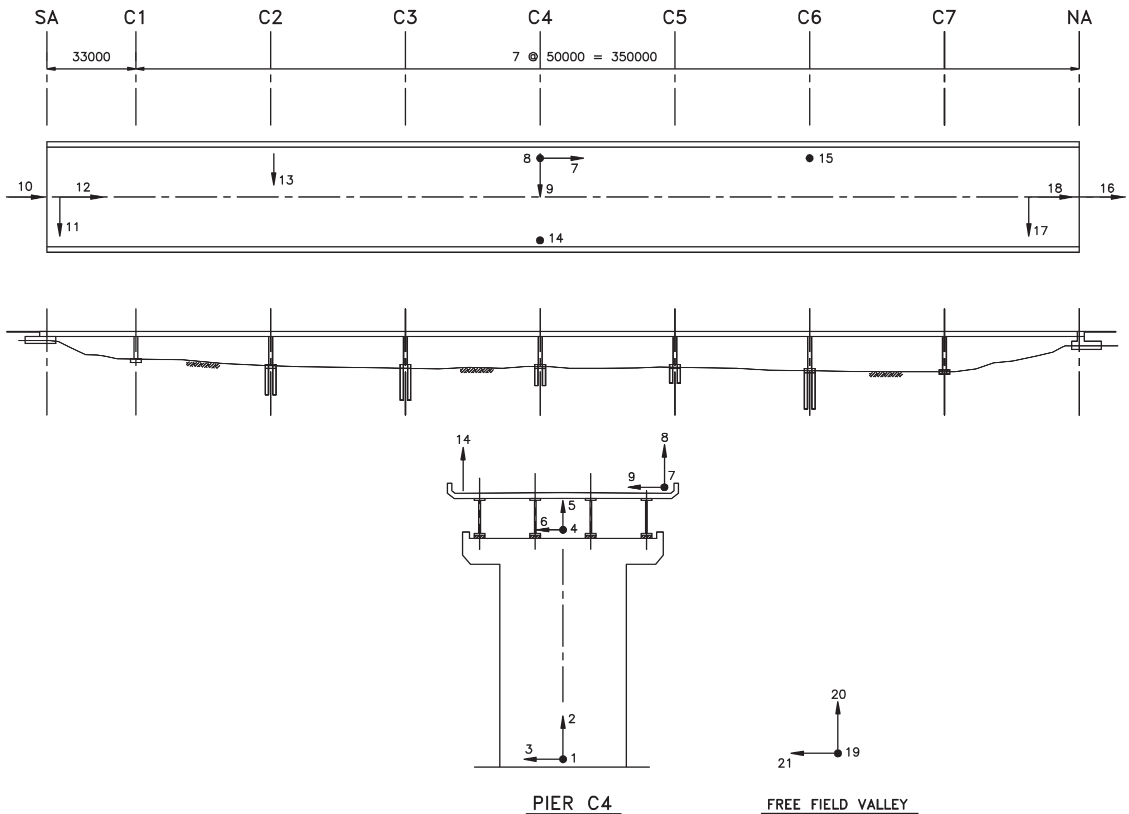

Fig. 6. Local acceleration network in Marga Marga Bridge.

Table 1
Natural frequencies and damping. Ambient vibrations and 24/07/2001 earthquake. Marga-Marga Bridge.

Ambient vibration			24/07/2001 earthquake		
Frequency (Hz)	Damping (%)	Predominant direction	Frequency (Hz)	Damping (%)	Direction sensor
1.05	2.6	Transverse	0.65	15	Longitudinal-deck
1.18	1.9	Transverse	0.85	3.4	Transverse-deck
1.5–1.7	1.2	Pier/Deck-General	1.25		Transverse-all
1.85	1.4	Trans-long	1.4–1.6		Longitudinal-all
1.8–2.1	1.5	Longitudinal	2.45–2.75	1.5	Vertical-deck

rubber pads and the conditions at the ends of the deck on the dynamic characteristics of the bridge using transfer functions in the frequency domain. For the rubber pads, with a shear modulus of 3.0 and 1.0 MPa, and free deck condition, significant peaks occurred at 0.5 Hz and 0.32 Hz in the longitudinal direction. This gives an starting point to prepare an analytical model of the bridge in order to reproduce the experimental data.

Displacements were obtained by double integration of the acceleration records, using standard software from Kinemetrics SMA, that includes a baseline correction of the records and filtering of low and high frequencies with a band pass between 0.15–0.25 Hz and 23.0–25.0 Hz, respectively. Maximum distortion of the bearings was 15.6 cm (76.5% rubber shear strain) and occurred in the transverse direction over pier C4. In the longitudinal direction, maximum distortion was about 11 cm (54% rubber shear strain) at the same location and around 6 cm at the abutments. For these shear strains, the G value would be 0.6–0.8 MPa, according to bearings tests.

Frequencies of 1.2 Hz, 1.0 Hz and 4.2 Hz were obtained at the "free-field valley" in longitudinal, transverse and vertical directions, respectively. The main difference with respect to ambient vibration measurements is in the vertical frequency of the soil.

3.3. Mathematical model

A finite element model of the bridge was developed using the Open Sees platform. Girders, slab and piers were represented by elastic beam–column type elements, and the isolators by elastomeric bearing type elements. In order to fit the experimental and analytical responses, the bearings stiffness were varied. The best result was obtained by the following properties: $ke=9.5$ kN/mm, $fy=40$ kN, $kf=2.0$ kN/mm; $ke=7.5$ kN/mm, $fy=11$ kN, $kf=0.75$ kN/mm and $ke=11$ kN/mm, $fy=20$ kN, $kf=1.1$ kN/mm, for the bearings located at the piers, south abutment and north abutment, respectively. Two different cases of input were considered. In the first, the records obtained at free field-valley were applied to the abutments and piers simultaneously in longitudinal, transverse and vertical directions. In the second model, records obtained at—south abutment were applied at south

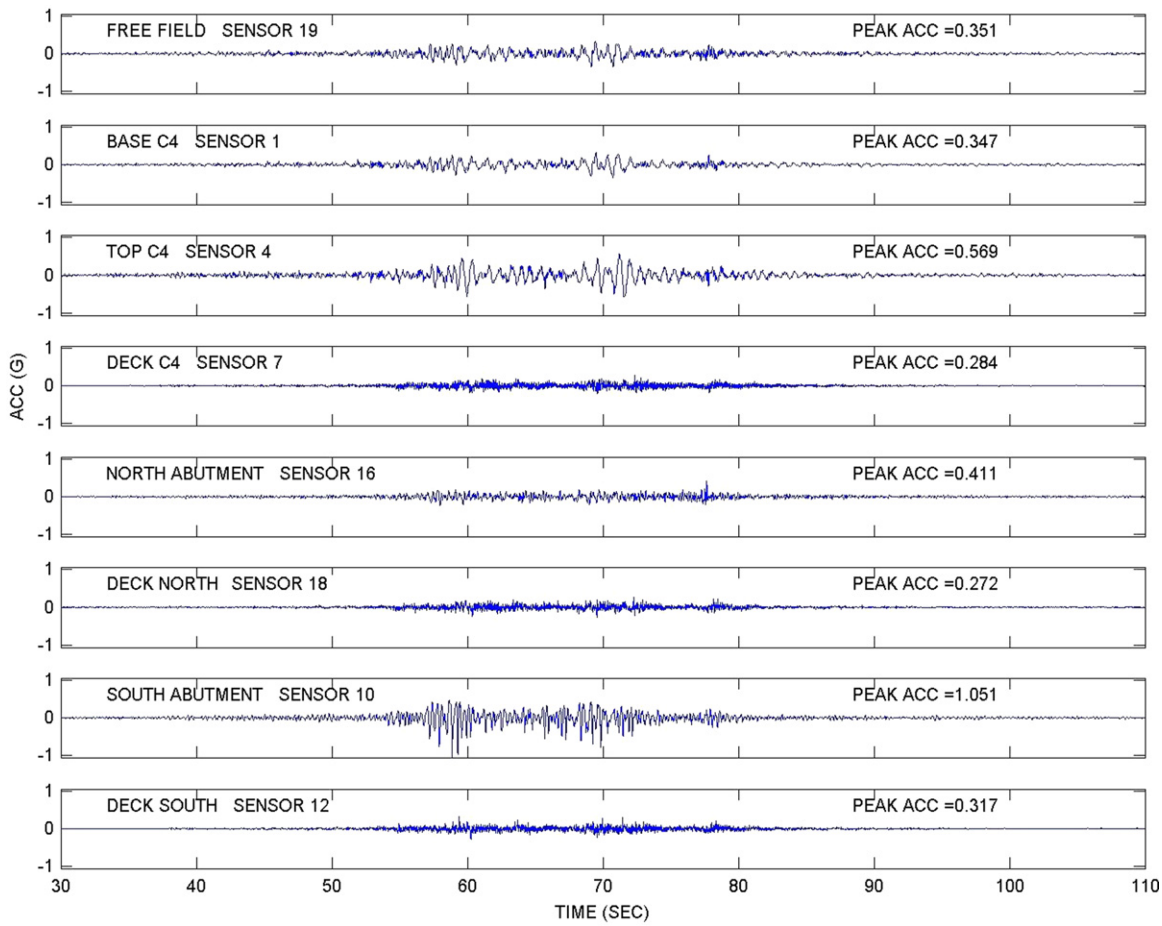

Fig. 7. Longitudinal records, 27/02/2010 earthquake. Marga Marga Bridge.

abutment and pier 1, records obtained at north abutment were applied at north abutment and piers 6 and 7, and the records from free field-valley were applied at base of piers 2–5, in longitudinal and transverse direction, while the vertical free field-valley record was applied at all the supports. All piers were considered fixed in all directions except the torsional direction that was free to move. Additionally, the deck was considered fixe at both abutments in transverse direction. Gap elements of elastic-perfectly plastic material were considered in longitudinal direction.

Rayleigh damping was used in both cases with 2% critical damping for modes 1 and 3. Figs. 13, 14 and 15 show theoretical and experimental displacements and spectral power densities obtained by longitudinal sensor 7, transverse sensor 9, and vertical sensors $(8+14)/2$, for both type of input. A significant improvement is observed with the use of non-synchronic motions at the supports.

Some factors that can explain the differences between theoretical and experimental results are: incorrect damping in the model, theoretical frequencies different from the experimental ones, differences in the input motions considered, between others.

4. Line 5, Santiago metro viaduct

4.1. Description

Line 5 viaduct of the Santiago Metro extends for 5,810 m, including stations: Rodrigo de Araya, Carlos Valdovinos, Camino Agrícola, San Joaquin, Pedrero and Mirador. The viaduct is composed of two 1.8 m high external prestressed concrete beams connected by means of a transversally post-tensioned concrete slab, 30 cm thick. The spans range from 27 to 36 m and widths from 6.3 to 7.5 m. The beams are simply supported on reinforced neoprene pads, 30×60 cm in plan and 5.2 cm thick, located at the ends of cantilevers spanning from a hollow central column. Column dimension are: 2.4×1.4 m and 30 cm thickness wall. At the stations, the columns are 2.4×2.2 m. The columns are connected monolithically to the foundations, which consist of a hollow reinforced concrete parallelepiped, with variable depth between 7 and 12 m, filled with compacted soil. Detailed information is in [12]. A view of a section and the station area is shown in Fig. 16a.

The instrumentation installed at the Metro Line 5 is a local network of three uniaxial and three triaxial accelerometers, as shown in Fig. 16b. Frequencies obtained in the longitudinal, transverse and vertical directions, from records of moderate earthquakes, are listed in Table 3.

4.2. Maule earthquake records

The Metro was able to operate normally after the quake, except for some minor damage to non-structural elements at some stations. Figs. 17–19 show the records obtained on February 27th, 2010 and also the square of the Fourier spectra of the motion in the longitudinal, transverse and vertical directions. Peak accelerations are listed at the right of each diagram. The reduction of acceleration in the longitudinal direction between the beam

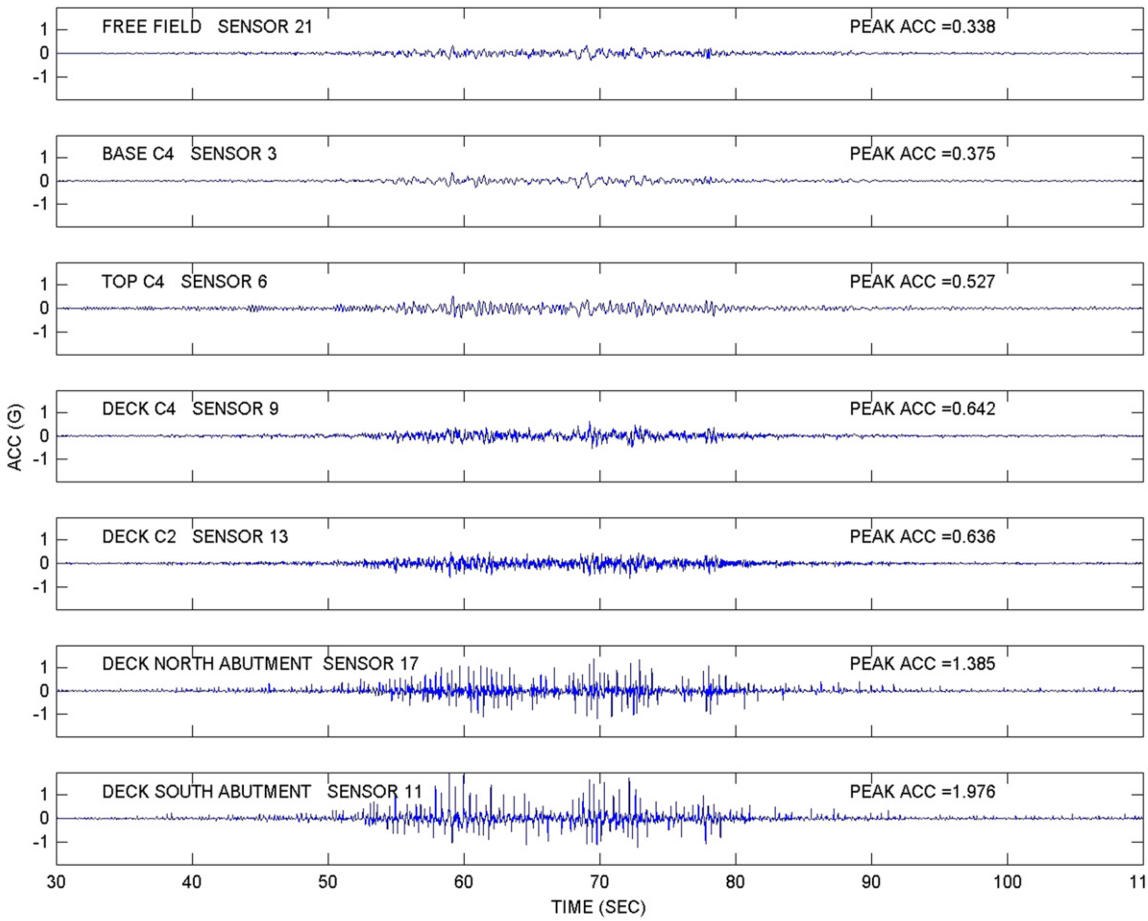

Fig. 8. Transverse records, 27/02/2010 earthquake. Marga Marga Bridge.

(sensor 4) and top of pier (sensor 8) is apparent. The acceleration in both horizontal directions at the pier top (sensors 8 and 9) is almost twice the acceleration at the bottom pier (sensors 10 and 11). The longitudinal acceleration is quite similar between the "free field" (sensor 1) and the pier bottom (sensor 11). Transverse accelerations at both ends of the beam (sensors 6 and 12) are very similar, which indicates the absence of torsion. The motion in the transverse direction on the deck shows quite different frequency content with respect to the pier top. Vertical acceleration at the deck almost double the pier top's and it is almost 2.5 the value at the free field.

The elastic acceleration spectra at the free field ground motions and the design spectrum are quite similar, as can be seen in Fig. 20.

Fourier spectra of sensors 1 and 11 are quite similar: it is hard to find any significant peak until 6 Hz, indicating that at both places the soil is quite rigid. At the pier top, the spectrum up to 2.2 Hz is quite similar to the pier bottom, but there is a peak of 24.1 at 2.52 Hz and a maximum peak of 33.6 around 7 Hz. At the beam (sensor 4) there is a maximum peak of 29.3 at 1.4 Hz. From 4 Hz up the energy is negligible. In the transverse direction, at the free field and pier bottom (sensors 3 and 10), up to 6.4 Hz, the energy is almost uniformly distributed in frequencies; the same can be observed in the longitudinal direction. From 7.3 Hz up the energy is negligible. At the pier top there is a maximum of 90 around 6.7 Hz. At the beam, sensors 6 and 12 coincide at a maximum peak of 116 for 1.25 Hz and a smaller one at 3 Hz. From 4 Hz up the energy is negligible. In the vertical direction, sensors 2 and 7 almost coincide, but on the beam, sensor 5 has a maximum peak of 203 for 2.5 Hz and a smaller one of 40 for 5 Hz. With this information, it is possible to identify some predominant frequencies and equivalent damping measured during this earthquake, which are shown in Table 4. The design frequency was 0.83 Hz, much lower than the values determined till now. Damping is quite low. It was obtained by means of the bandwidth method [13].

Integrating twice the acceleration records, the maximum shear deformations at the bearings were determined. They were 2.2 cm and 2.7 cm in longitudinal and transverse directions, which correspond to 56% and 67% of shear strain. These values are lower than the 3 cm considered as the designed maximum allowed displacements. [14].

4.3. Mathematical model

A three-dimensional model was developed using SAP2000 that included frame elements representing the piers and superstructure, and rubber isolator elements representing the bearings. Lateral springs were used to represent the soil confinement. Three continuous span were considered, the span at the left, which is closer to Mirador Station, is 27 m long, while the span length of the other two is 36 m. The height of the columns is 8 m. In order to fit the model to the predominant frequencies determined experimentally from the earthquake records, the piers, bearings and soil spring stiffness were varied. Changes in bearing stiffness affected the vibration modes containing deck movements; changes in the soil stiffness affected mainly the modes containing piers' movements; and changes in the mechanical

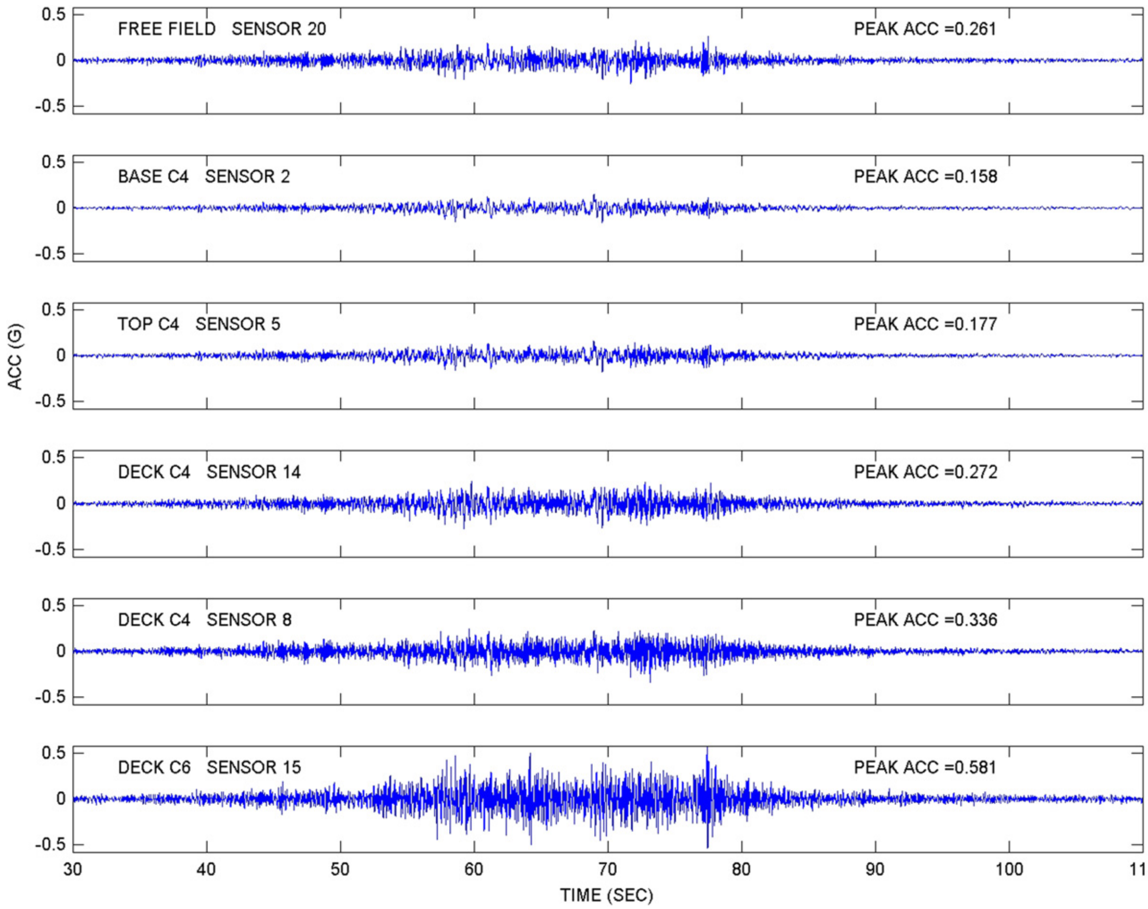

Fig. 9. Vertical records, 27/02/2010 earthquake. Marga Marga Bridge.

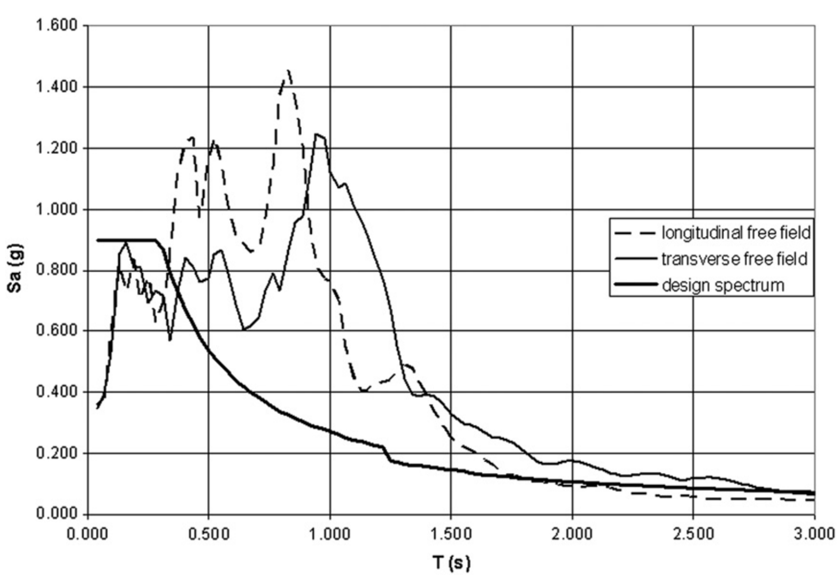

Fig. 10. Elastic response spectra, Marga Marga bridge.

properties of the concrete affected mainly the modes containing vertical movements. The best result was obtained for ''high soil spring stiffness'' and about 8% rubber shear distortion, (G=2.0 MPa). Theoretical frequencies are also shown in Table 4.

Modal damping was varied to fit acceleration and displacement time history records. The best fit was obtained for damping much higher than the one estimated with the half band-width method.

5. Conclusions

Despite the magnitude of the February 27th, 2010 earthquake, most road structures had an adequate performance. However, while less than 0.15% of the exposed structures in the stricken area were damaged or unserviceable, there was a critical situation for surface transportation, which was vital for assisting the affected communities.

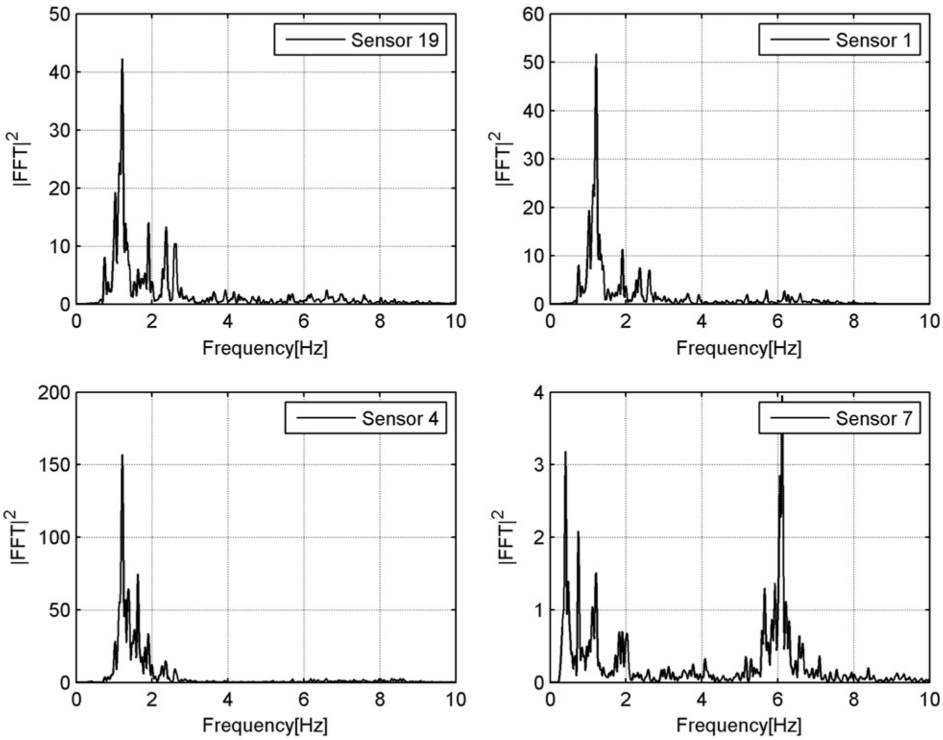

Fig. 11. Square Fourier Spectra, 27/02/2010 earthquake. Marga Marga Bridge.

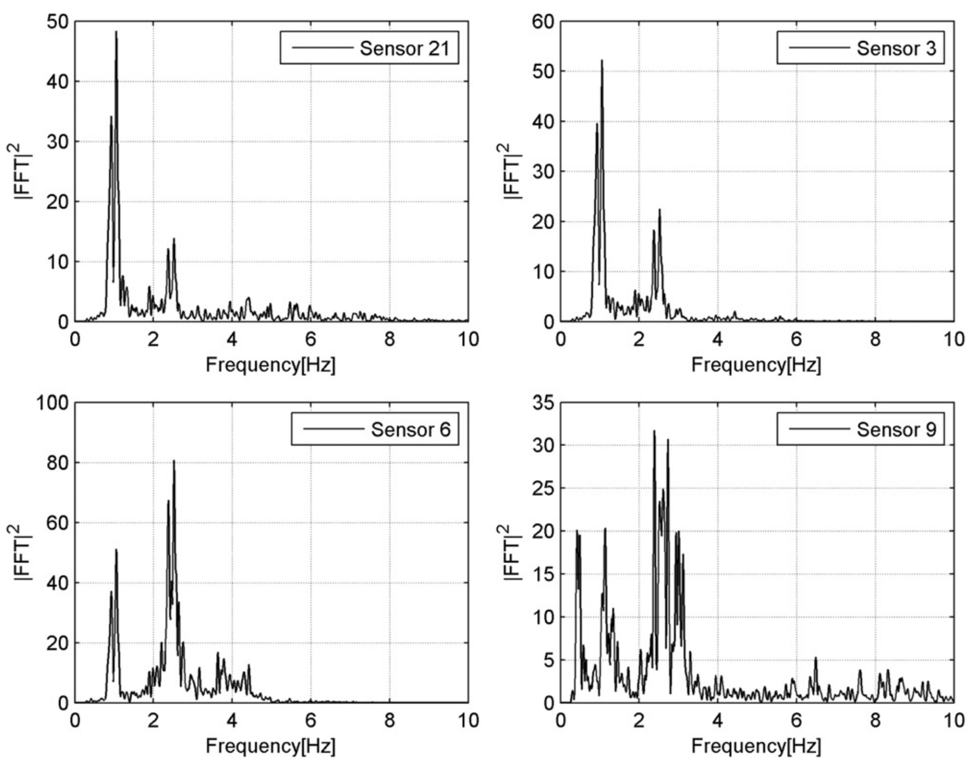

Fig. 12. Square Fourier Spectra, 27/02/2010 earthquake. Marga Marga Bridge.

As a consequence of the damage observed in different types of bridge during the February 27th, 2010 earthquake, the Ministry of Public Works elaborated a document that corrects the Chilean code for structural design of bridges, increasing the requirements for new bridges [15]. The main changes were related to seating length at abutments, piers, and joints of girders, seating length at abutments for skew bridges, and unseating prevention structures connecting the superstructure with the substructure. In all these cases the new specifications were taken from the Japanese code [16]. Additional specifications are related to the size of

Table 2
Frequency analysis, Marga Marga Bridge, 27/2/2010 earthquake.

Interval	Direction	Sensor*	Frequency (Hz)	Damping (%)	Comments
1 (0–50.4 sec)	Longitudinal	pier top	1.42–1.55		
		deck	0.57–0.66	9–10	
	Transverse	pier top	1.16		
		deck	0.75		
2 (50.4–84.8 sec)	Longitudinal	deck	0.40	6.3	Strong motion interval
		deck	0.75	3.6	
		all	1.21		
	Transverse	deck	0.43–0.48	11.4–12	
		all	0.93		
		all	1.05		
	Vertical	all	1.2–1.29		
		deck	2.37–2.64		
3 (84.8–170 sec)	Longitudinal	deck	0.49	19.5	Signal decay
		all	1.14–1.4		
	Transverse	all	1.21		

* This column indicates the location of the sensors that contribute with energy to each mode, i.e, in longitudinal direction, pier top represents sensor 4 and deck represents sensors 7, 12 and 18.

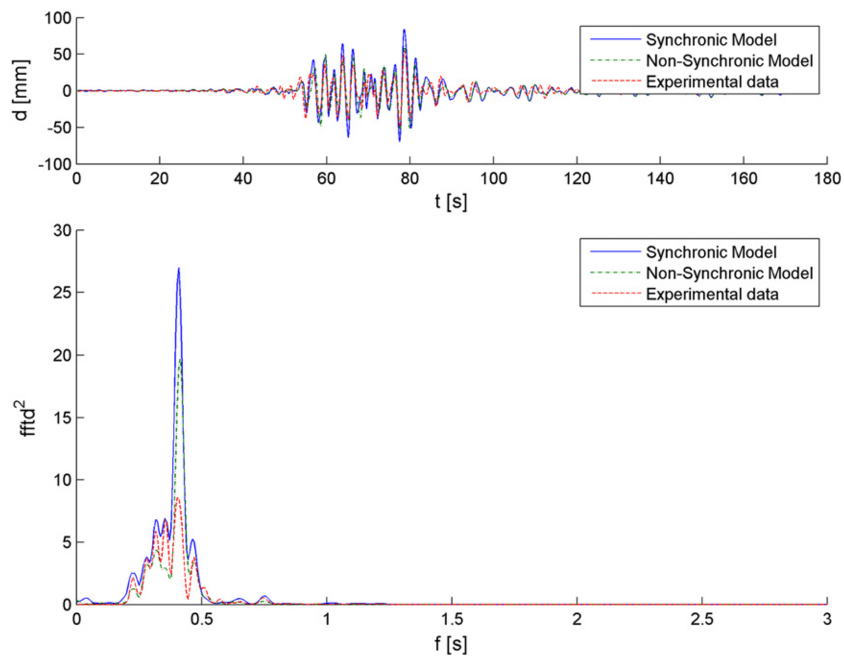

Fig. 13. Comparison between experimental and theoretical response, Marga Marga Bridge, longitudinal direction.

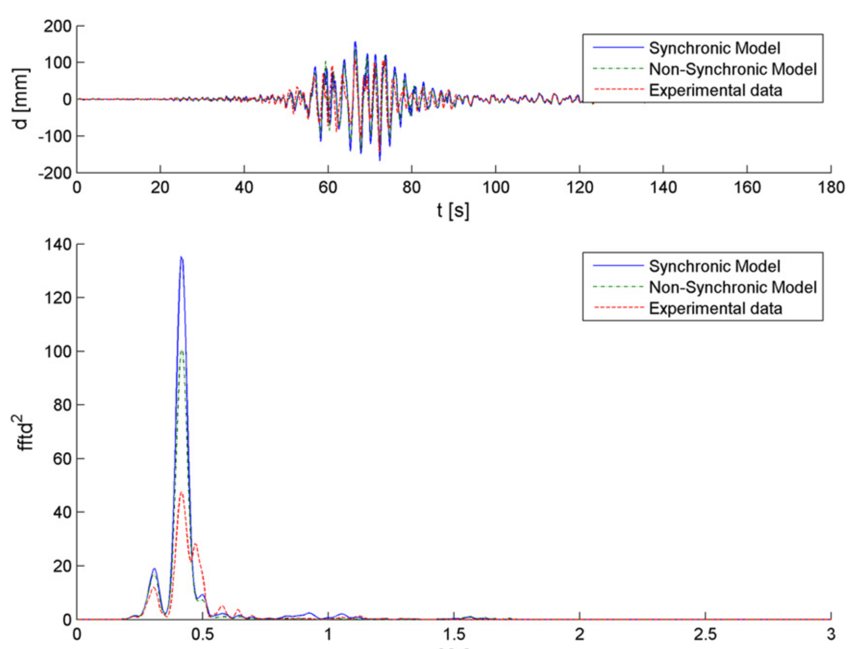

Fig. 14. Comparison between experimental and theoretical response, Marga Marga Bridge, transverse direction.

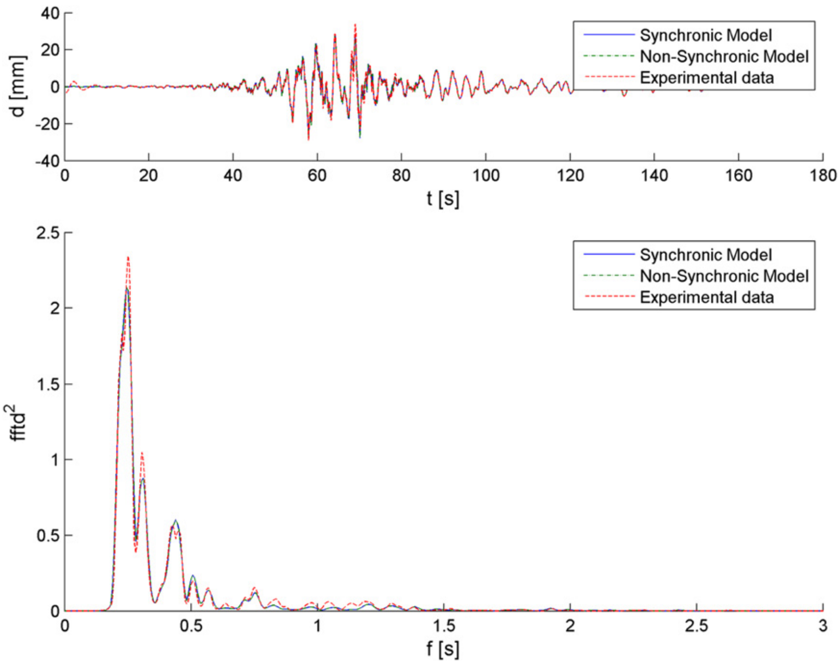

Fig. 15. Comparison between experimental and theoretical response, Marga Marga Bridge, vertical direction.

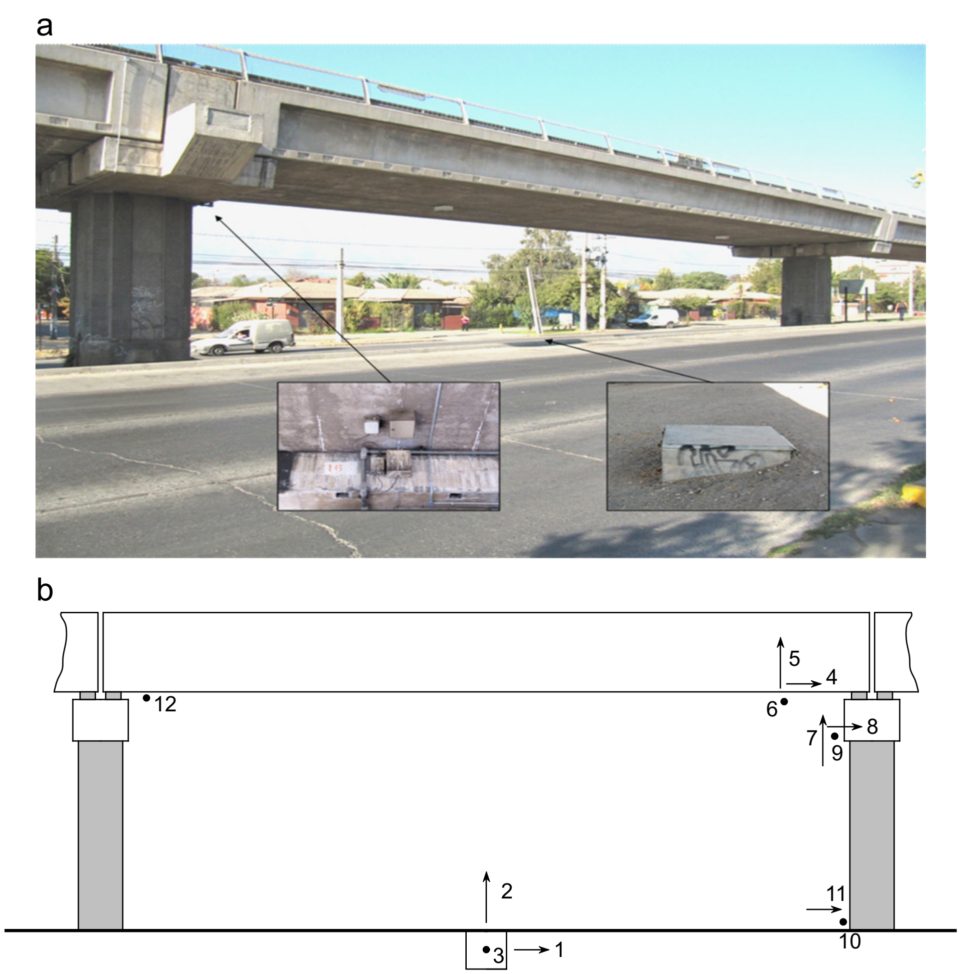

Fig. 16. General view, Line 5 viaduct and Local acceleration network in Line 5 viaduct.

Table 3
Frequency analysis, moderate earthquakes. Line 5 metro viaduct.

Mode	Direction	Frequency (Hz)	
		Minimum	Maximum
1	Longitudinal	1.5	2.6
2	Transverse	1.4	2.4
3	Vertical	2.6	3.1

temperature joints, vertical anchorage bars at abutments and the compulsory use of transverse diaphragms between girders at the abutments and at the center of span.

The seismically isolated structures had good performance, and thanks to the instrumentation installed in some of them, important information about their response to severe earthquakes was obtained for the first time. In general, there were significant reductions in the longitudinal directions of the bridges and,

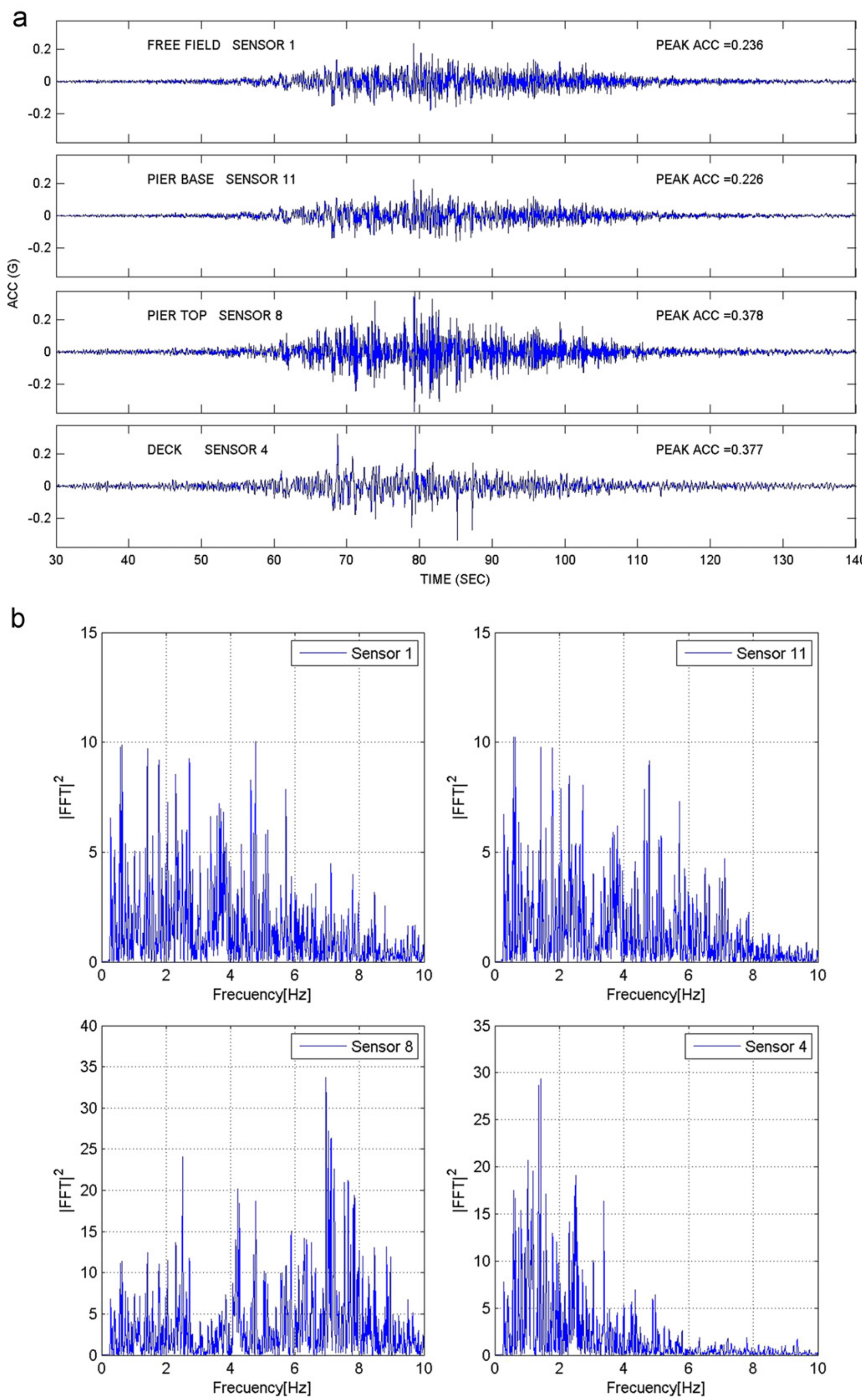

Fig. 17. Longitudinal acceleration records and square Fourier spectra, 27/02/2010 earthquake. Line 5 viaduct.

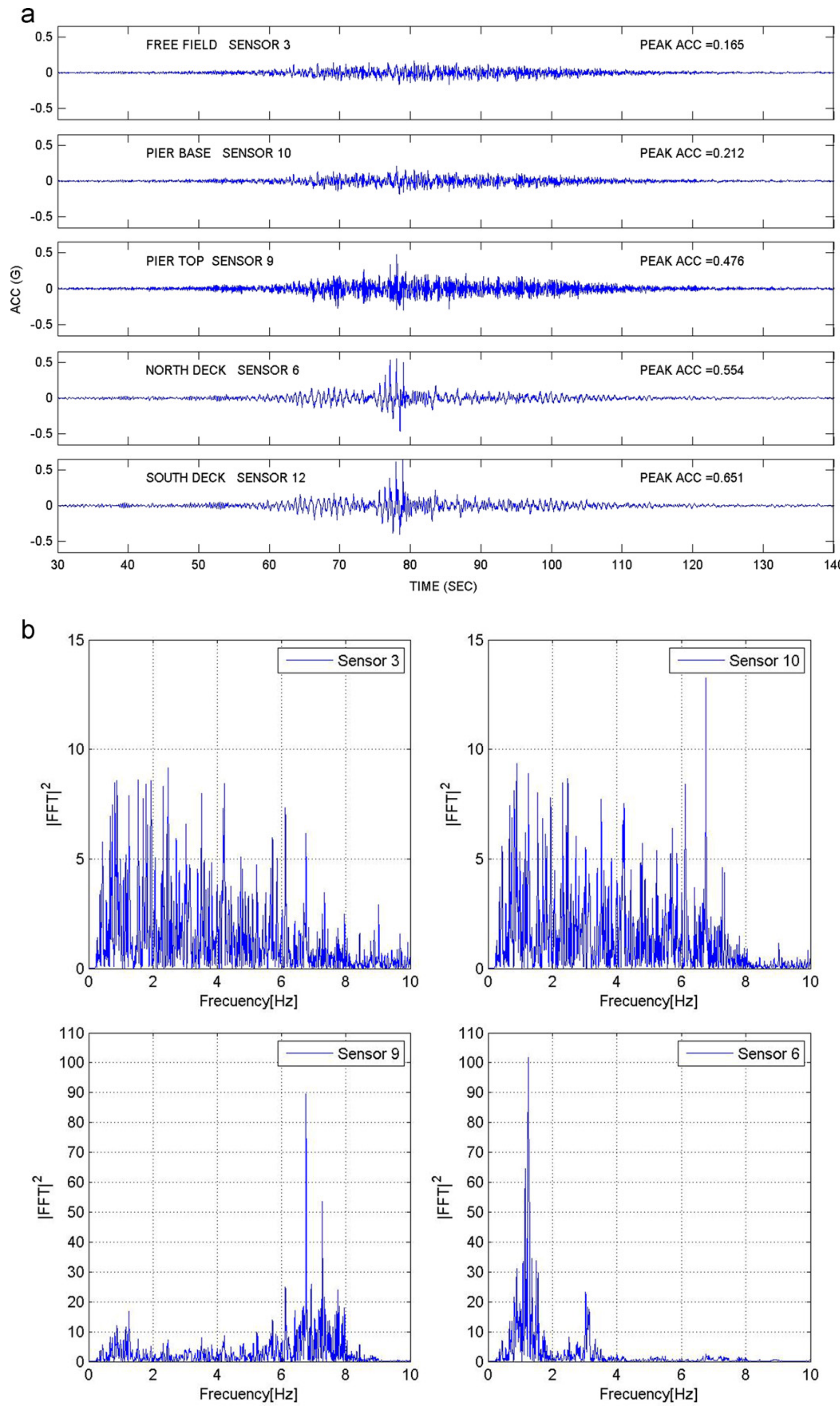

Fig. 18. Transverse acceleration records and square Fourier spectra, 27/02/2010 earthquake. Line 5 viaduct.

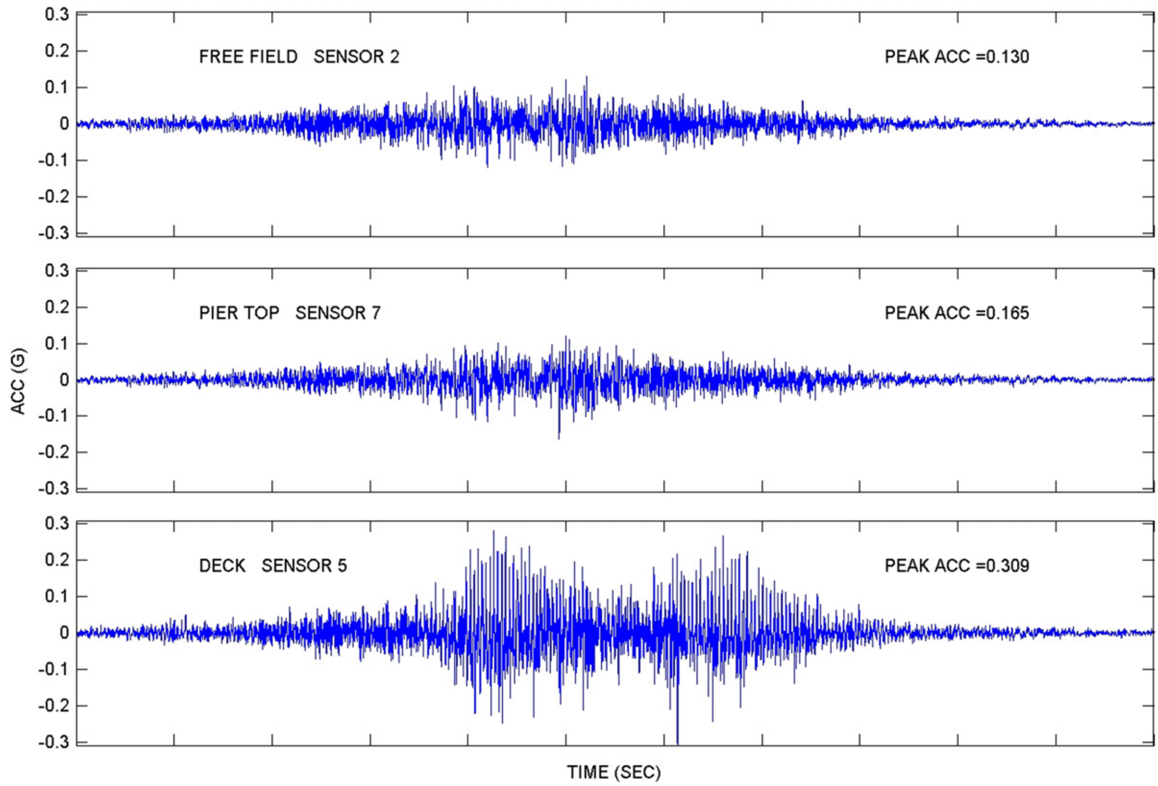

Fig. 19. Vertical acceleration records and square Fourier spectra, 27/02/2010 earthquake. Line 5 viaduct.

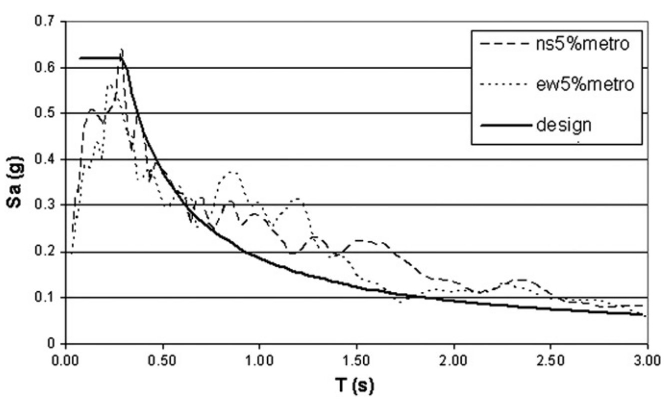

Fig. 20. Design and elastic response spectra, Metro.

Table 4
Frequency analysis, 27/02/2010 earthquake, Line 5 Metro Viaduct.

Mode	Direction	Experimental		Theoretical
		Frequency (Hz)	Damping (%)	Frequency (Hz)
1	Transverse	1.25	1.8	1.32
2	Longitudinal	1.4	0.8	1.26
3	Vertical longitudinal	2.5	0.5	2.57
4	Transverse	3.0	0.6	2.36
5	Vertical	5.0	0.2	5.79

although vertical movement was amplified, this fact was not critical for the structures. Bearings didn't show any sign of distress.

The frequency responses of the bridges have been predicted by computational models. For the Marga Marga Bridge, non-synchronic input motions had to be considered. Modal damping is very hard to evaluate. Marga Marga Bridge and Metro viaduct performed as expected during the design phase.

Acknowledgments

This research was made possible by the financial support from the Universidad de Chile, the Ministry of Public Works (MOP), Metro de Santiago and Fondecyt, which have provided funding for equipment, installation, and maintenance during more than a decade. Additional support was provided by CONICYT-Chile postgraduate fellowship program to Braian Venegas, Master Student at University of Chile.

Appendix A. Supporting information

Supplementary data associated with this article can be found in the online version at http://dx.doi.org/10.1016/j.soildyn.2012.06.019.

References

[1] Barrientos S. Earthquake Cauquenes, February 27, 2010. Technical Report Updated May 27, 2010, 〈http://ssn.dgf.uchile.cl〉; 2010.
[2] Boroschek R, Soto P, León R, Comte D. Terremoto Centro Sur, 27 Febrero 2010. Informe Preliminar No. 4, 〈www.renadic.cl〉; 2010.
[3] Kunde MC, Jangid RS. Seismic behaviour of isolated bridges: a-state-of-the-art review. Electronic Journal of Structural Engineering 2003;3.
[4] Chaudhary M. Evaluation of seismic performance of base-isolated bridges based on earthquake records. PhD dissertation. Department of Civil Engineering, Japan: University of Tokyo; 1999.
[5] Huang MC, Wang YP, Chang JR, Chang Chien CS. Physical system identification of an isolated bridge using seismic response data. Structural Control and Health Monitoring 2009;16:241–65.
[6] Moroni MO, Sarrazin M, Benavides C, Díaz A. Características dinámicas de puentes chilenos con protección sísmica. Revista Sul-Americana de Engenharia Estructural, Passo Fundo 2004;1(2):55–73.

[7] Hube M, Santa María H, Villalobos F. Preliminary analysis of the seismic response of bridges during the Chilean 27 February 2010 earthquake. Obras y Proyectos 2010;8:48–57.
[8] Yen W, Chen G, Buckle I, Allen T, Alzamora D, Ger J, et al. Post earthquake Reconnaissance Report on Transportation Infrastructure Impact of the February 27, 2010, offshore Maule Earthquake in Chile, FHWA-HRT-11-030. US Department of Transportation; 2011.
[9] Boroschek R, Moroni MO, Sarrazin M. Dynamic Characteristics of a long span seismic isolated bridge. Engineering Structures 2003;25:1479–90.
[10] Taylor D, Trigo T, Moroni MO, Sarrazin M., Análisis dinámico del puente Marga–Marga considerando variación espacial del movimiento sísmico. In: Proceedings of the XXXIII Jornadas Sudamericanas de Ingeniería Estructural; 2008.
[11] Dai W, Moroni MO, Roesset JM, Sarrazin M. Effect of isolation pads and their stiffness on the dynamic characteristics of bridges. Engineering Structures 2006;28(9):1298–306.
[12] Sarrazin M, Moroni MO, Romo D, Quintana J, Soto P. Respuesta sísmica de puentes chilenos con apoyos aislantes. Revista Internacional De Desastres Naturales, Accidentes e Infraestructura Civil 2002;2(2):31–48.
[13] Tanaka T, Yoshizawa S, Osawa Y, Morishita T. Period and damping of vibration in actual building modes. Bulletin of the Earthquake Research Institute 1969;47:1073–92.
[14] Sarrazin M, Saragoni R, Araya M, Gonzalez A, Izzo F, Vergara R. Applications of seismic isolation to the Santiago metro, line 5 and the Rodelillo Viña Del Mar highway bridge. In: Proceedings of the international post-smirt conference seminar on seismic isolation, passive energy dissipation and control of vibrations of structures, Santiago, Chile; 1995. pp. 431–44.
[15] Nuevos Criterios Sísmicos para el Diseño de Puentes en Chile. Department of Projects and Structures, Engineering Division, Roads Direction, Ministry of Public Works; 2011.
[16] Specifications for Highway Bridges, Part V Seismic Design. Japan; 2002.